Exchange-correlation effects in ballistic and dissipative transport in GAA Si nanowire transistors

A. Martinez[1], M. Aldegunde[2], K. Kalna[1], J. R. Barker[3]
[1]College of Engineering, Swansea University, Singleton Park, Swansea SA2 8PP, Wales, UK
[2] Supercomputer Centre of Galicia, 15705 Santiago de Compostela, Spain
[3]School of Engineering, University of Glasgow,UK
Email: a.e.martinez@swansea.ac.uk

Many-body effects such as dynamic image charge [1] and exchange-correlation [2] affect electron energy levels in the channel of a nanotransistor, as a large surface/volume ratios and high electron densities are achieved inside the device. The impact of exchange and correlation (XC) on inversion layers [3-4] and on the current-voltage characteristics for 2D device architectures [5] such as double gate, have been investigated in the context of ballistic or semi-classical transport. Furthermore, looking ahead to more predictive device simulations, the quantitative assessment of these effects will become of paramount importance. Nanowire transistors and other 3D architectures have become increasing relevant for the semiconductor industry, as FinFet devices have already been integrated in microprocessor technology by INTEL corporation. In this work we investigated the impact of the exchange correlation in the I_D-V_G characteristics as a function of the nanowire cross section using a Non Equilibrium Green Function (NEGF) formalism [6, 7]. Gate-all-around (GAA) nanowire transistors with 2.2x2.2 nm^2 and 3.6x3.6 nm^2 cross section have been studied. Ballistic and dissipative (phonon scattering) simulations have been carried out. The nanowires have 14 nm S/D and 10 nm channel length and a 0.8 nm SiO_2 thickness. The channel is considered un-doped and the S/D has a *n*-type doping concentration of 10^{20} cm^{-3}. The drain bias is set to 100mV. The Hamiltonian is written in the effective mass approximation [8] and XC is implemented in the interpolated local density approximation of Hedin [2]. We used the phonon scattering model from reference [9]. Fig. 1 shows the I_D-V_G for the ballistic and dissipative simulations with/without XC for the 2.2x2.2 nm2 device. The XC potential lowers the source-to-drain barrier resulting in a large drain current as shown in Fig. 2 (conduction band profile for the 2.2x2.2 nm2 device at VG=0.7 V). The XC potential has a negligible impact in the sub-threshold region, as the electron concentration in the channel is low. Fig. 3 shows the drain current increases as a function of the gate bias. The shape of the curve is the result of an interplay between source-to-drain tunneling, which tends to minimize the impact of the XC and the electron density in the channel tend to maximized the effect XC. The XC potential increases the drain current by almost 50%. The spectrum of the current for a 2.2x2.2nm2 (3.6x3.6 nm2) device with XC and phonon scattering is shown in fig. 4 (fig.5). There is a large effective electron-phonon coupling for the small cross section device, as compared with the large one. This results in a large spread in the current and the quick relaxation of the electron at the drain in fig.4 as compared to fig. 5. There is significant tunneling in both cases as the channel length is 10 nm but the electrons in the large cross section devices have lower effective masses and therefore large tunneling probability. Fig. 6 shows the I_D-V_G for the ballistic and dissipative simulations with/without XC for the 3.6x3.6 nm2 device. The corresponding current enhancement is shown in fig. 7. The effects of the XC in the I_D-V_G are qualitatively similar to the case of the small cross-section device but the effect is lower (30%) as the tunneling is stronger

REFERENCES

1] C. Li, M. Becond, M. Lannoo, Phys RevB **80**, 195318 (2009).
[2] L. Hedin et al J. Phys. C: Solid St. Phys. **4**, 2064-83 (1971).
[3] D. Vasileska et al, IEEE Trans. Electron Dev **44**, 584-1587 (1997)
[4] H. Iwata,etal, IEEE Trans. Electron Dev **52**, 1596-1602 (2005).
[5] Matthias Sabathil, PhD thesis, unpublished, Munich technical University (2004). [6] L. V. Keldysh JETP, 47, 1515-1527 (1964),
[7] A. Svizhenko et al., J. Appl. Phys. **91** (4), 2343-2354 (2002).
[8] A. Martinez et al IEEE Trans. Electron. Dev 54(9) 2213-2222 (2007). [9] M. Aldegunde et al. J. Appl. Phys. **110**, 094518 (2011);

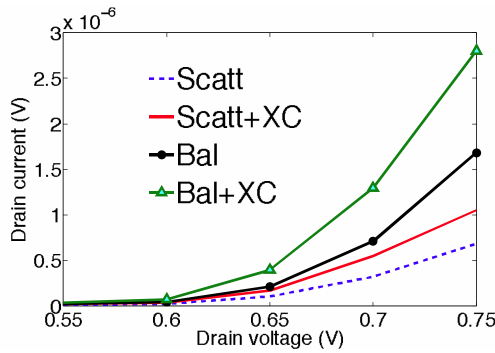

Fig. 1. I_D-V_G characteristics for the 2.2x2.2 nm^2 cross-section device (Vd=0.1 V).

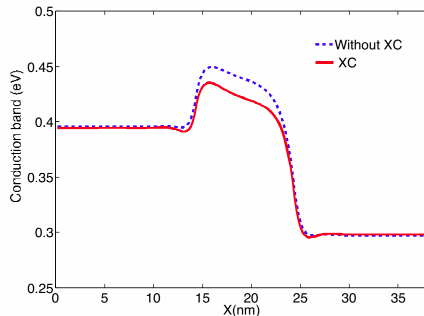

Fig. 2. First sub-band for the ballistic 2.2x2.2nm^2 cross-section device at Vg=0.7 V

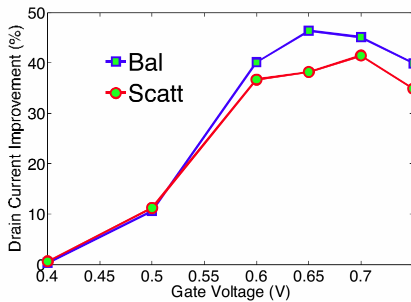

Fig. 3. Current improvement due to XC effects in the devices of fig. 1.

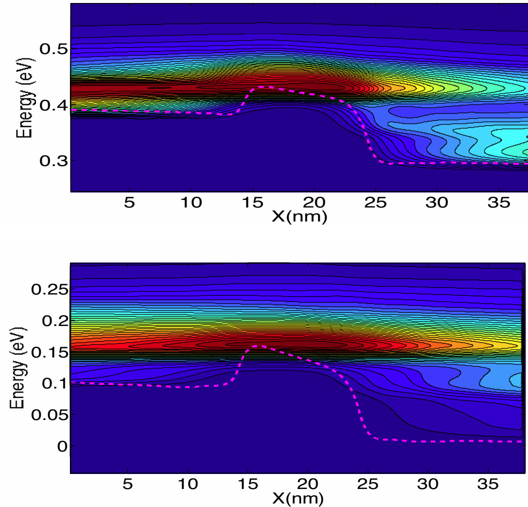

Fig. 4. Current spectra along the channel. Upper panel for the 2.2x2.2nm^2 device with scattering and XC. Lower panel for the 3.6x3.6nm^2 device with scattering and XC

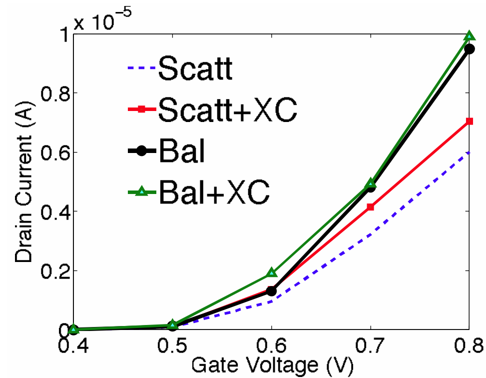

Fig. 5. I_D-V_G characteristics for the 2.2x2.2 nm^2 cross-section device (Vd=0.1 V).

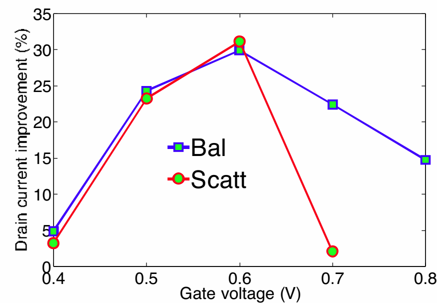

Fig. 6. Current improvement due to XC effects for the devices of Fig. 5.